

## Relaxors as superparaelectrics with distributions of the local transition temperature

This article has been downloaded from IOPscience. Please scroll down to see the full text article.

1995 J. Phys.: Condens. Matter 7 4145

(<http://iopscience.iop.org/0953-8984/7/21/013>)

View [the table of contents for this issue](#), or go to the [journal homepage](#) for more

Download details:

IP Address: 171.66.16.151

The article was downloaded on 12/05/2010 at 21:22

Please note that [terms and conditions apply](#).

# Relaxors as superparaelectrics with distributions of the local transition temperature

A E Glazounov, A J Bell and A K Tagantsev

Laboratoire de Céramique, EPFL, CH 1015 Lausanne, Switzerland

Received 19 December 1994, in final form 6 March 1995

**Abstract.** A model of relaxors as superparaelectrics with a distribution of the local transition temperature has been investigated. The necessary model parameters are obtained from the analysis of the static polarization response of lead magnesium niobate and then employed in simulations of the frequency-dependent dielectric properties.

The present model is compared with a previously published model of relaxors, based on a single transition temperature but with a distribution of the size of the polar regions. Both of them describe some characteristic features of relaxors, i.e. the shift of the peaks in temperature dependence of the real and imaginary parts of the dielectric permittivity with frequency and the broadening of the relaxation time spectrum on cooling. However, a model which takes into account the distribution of the size of the polar regions describes qualitatively correctly the shape of the relaxation time spectrum.

## 1. Introduction

Relaxor ferroelectrics (or relaxors) attract much interest, from the viewpoint of both practical applications and pure science. Amongst these compounds, lead magnesium niobate  $\text{Pb}(\text{Mg}_{1/3}\text{Nb}_{2/3})\text{O}_3$  (PMN) is considered as a model material, and, therefore, has been the focus of much research during the last thirty years.

The basic dielectric properties of PMN, in both ceramic and single-crystal form, have been reported by Smolensky *et al* [1], and Bokov and Myl'nikova [2], respectively. The temperature dependence of the relative dielectric permittivity,  $\epsilon'$ , of PMN has a broad peak. The temperature of the peak ( $T_{\text{max}}$ ) and its magnitude ( $\epsilon'_{\text{max}}$ ) depend upon the frequency  $\omega$  of the applied electric field in the radiofrequency range. With increasing  $\omega$ ,  $T_{\text{max}}$  shifts toward higher temperatures and  $\epsilon'_{\text{max}}$  decreases. Below  $T_{\text{max}}$  the dielectric permittivity of PMN displays strong relaxation dispersion in the radiofrequency range. At low temperatures, the macroscopic polarization,  $\mathbf{P}$ , as a function of the electric field,  $\mathbf{E}$ , shows a large hysteresis, which decreases with increasing temperature and disappears close to  $T_{\text{max}}$ . For temperatures higher than  $T_{\text{max}}$ , polarization is a single-valued non-linear function of the field. Since that time much information about the properties of PMN, at temperatures both above and below  $T_{\text{max}}$ , has been published.

The dielectric properties of relaxors are generally explained in the literature in terms of small polar regions. The latter are defined as separate regions of the crystal which have nanometre scale size and possess spontaneous polarization. The dielectric response is interpreted as a result of reorientation of the local polarization vectors ( $\mathbf{P}_s$ ) under applied electric field. However, an origin of the polar regions and how they control the dielectric properties of relaxors as a function of temperature and frequency are still matters of debate.

Several attempts have been made to model the dielectric response of relaxors using various hypotheses concerning the origin and behaviour of the polar regions.

Smolensky and Isupov originally introduced a concept of the 'diffuse phase transition', resulting from composition fluctuations on a microscopic scale (this model is mostly known from the review given by Smolensky [3]). The phase transition into the polar state occurs in separate regions of the crystal, with a size of 100–1000 Å, independent of one another, with the local transition temperature,  $T_c$ , depending upon the composition of the individual region. The dielectric response was interpreted as a switching of the local spontaneous polarization between states with different orientations of the vector  $P_s$ . At a given temperature  $T$ , only regions of which the local  $T_c$  is close to  $T$  contribute to the macroscopic dielectric response, since the activation energy required to switch the polarization in the region increases drastically with temperature below  $T_c$ . Kirillov and Isupov [4] attempted to model the dielectric permittivity of PMN using this concept of the temperature dependence of the number of relaxing regions. Even though they obtained a good fit to the dielectric permittivity as a function of temperature, the frequency dispersion was not described well. In their model dielectric relaxation is of Debye-type; however, Cole–Cole plots suggest a broad distribution of relaxation time [1].

Cross [5] suggested that relaxors might be considered as superparaelectrics. He visualized them as consisting of small non-interacting polar regions each with a local spontaneous polarization. Cross postulated that since ferroelectricity is a cooperative process, the energy involved with every polar region must scale with volume and that for regions with a size of  $\sim 100$  Å the potential barrier required to reorient the local polarization vector would be comparable to the thermal energy of the crystal. Thus, the local polarization in each region can fluctuate under the thermal agitation. According to this model all the polar regions contribute to the orientation polarization, and, on cooling, the temperature and frequency dependence of dielectric permittivity is due to slowing down of the fluctuations of the local polarization vectors.

Viehland *et al* [6] tried to fit electric field dependences of the polarization in a wide temperature range from below  $T_{\max}$  to high temperatures. In their model relaxors were formally compared with magnetic spin glasses and were envisaged as consisting of interacting polar regions, with polarization fluctuations occurring above the static freezing temperature.

Recently Bell [7] proposed a method for calculation of the dielectric properties of a superparaelectric. The approach was to treat individual polar regions as classical ferroelectrics and employ the Landau–Ginsburg–Devonshire (LGD) theory of ferroelectrics to describe the temperature dependence of their parameters. Unlike the Smolensky and Isupov model [3], he used a single transition temperature and implied that the whole volume of the crystal is occupied by the polar regions. The calculations were performed for the fictional superparaelectric  $\text{Pb}(\text{Zr}_{0.7}\text{Ti}_{0.3})\text{O}_3$ . Bell [7] compared several possible scenarios of dielectric behaviour and in some cases attained a good resemblance to the observed behaviour. Particularly good results were obtained when a distribution of the sizes of the polar regions was introduced into the calculations. In subsequent work [8] an attempt was made to use the same approach and simulate the dielectric response of PMN taking the numerical values of the model parameters estimated from the experimental evidence for this material. Despite some discrepancies, the model appeared to give satisfactory results for the dielectric permittivity in the temperature range around  $T_{\max}$ .

It is a characteristic of relaxors that their dielectric properties are controlled by a broad spectrum of relaxation times [9–11]. In [7] the spectrum was brought about by the distribution of the sizes of the polar regions. However, there is another possible origin

of the spectrum of relaxation times, namely, the distribution of local transition temperatures. This second possibility has not yet been fully tested.

The purpose of this paper is to explore a model which considers relaxors as superparaelectrics with a distribution of local transition temperatures and to clarify how well the latter may account for the dielectric properties of these materials. The model will be introduced in the second section of the paper, using PMN as a model material. As a first test we shall fit the static polarization of PMN as a function of the applied electric field and temperature to the model. An approach to data analysis, the experimental part and the results of the fitting will be presented in the third, fourth and fifth sections of the paper, respectively. Then the model will be tested again through the simulations of the dielectric response, both static and dynamic, of relaxors in a wide temperature range, and comparison of the results of the simulations with the experimental data. The calculations will be carried out using the results of the analysis of the experimental data reported in the fifth section.

## 2. The model

The model presented in this paper is based on three well known ideas.

(a) Chemical heterogeneity, which is a common characteristic of all relaxors, plays the key role in the formation of microscopic polar regions [3]. As similar cations ( $Mg^{2+}$  and  $Nb^{5+}$  in the case of PMN) are randomly distributed in the crystal lattice, it may happen that on the microscopic scale there exist regions within which the concentrations of  $Mg^{2+}$  and  $Nb^{5+}$  are constant, but differ from one region to another. It is reasonable to expect that this scale is of the order of 10 to 1000 Å—larger than the size of the unit cell, but much smaller than the size of the crystal or a single ceramic grain. A distribution of the composition of such regions results in  $T_c$ , temperature of the transition into a polar state, varying from one region to another.

(b) These microscopic regions are independent from each other [3, 5].

(c) The small size of the regions makes it possible to reorient the direction of the local polarization vector rather easily, unlike the normal ferroelectrics [5]. That is, below the local transition temperature each region behaves as a single dipole moment.

The model considers relaxors as an ensemble of non-interacting polar regions. The polar regions have a finite size  $l$ , which is equal for all the regions. Each region behaves as an independent, normal ferroelectric with a local transition temperature  $T_{c,i}$ , below which it possesses local, temperature-dependent, spontaneous polarization  $P_{s,i}$ . For convenience we introduce here a dipole moment  $p_i$  of the individual region, which is given by  $p_i = P_{s,i}l^3$ . There is a distribution of the local transition temperatures, and the number of polar regions, thus, changes with temperature. At a given temperature  $T$ , the total number of the polar regions is  $n_T$ , and they occupy only a certain part of the crystal. On cooling, new polar regions appear, and their number and volume fraction in the crystal increase. The rest of the crystal volume is considered as a dielectric with isotropic properties (it is usually said that the polar regions are embedded in an isotropic dielectric matrix). Structural data [12] suggest that the polar phase has rhombohedral symmetry. As the polar regions do not interact with one another the local polarization vectors in different regions are randomly oriented in the eight  $\langle 111 \rangle$  pseudocubic directions allowed by the rhombohedral symmetry. Thus, in the absence of the external electric field the crystal is macroscopically isotropic and the macroscopic polarization is equal to zero.

### 2.1. Dielectric response of relaxors

There are two contributions to the macroscopic dielectric response of relaxors: orientation and high-frequency polarization. The latter represents the pure response of the crystal lattice to the applied electric field and is characterized by the high-frequency dielectric permittivity  $\epsilon_\infty$ . Orientation polarization results from the alignment of vectors of the dipole moments of individual regions parallel to the direction of the applied electric field.

In the static case each polar region contributes to the orientation polarization a component  $\langle p_i \rangle$  in the direction of the applied field. For the polar regions with rhombohedral symmetry the value of  $\langle p_i \rangle$  can be written [7] as

$$\langle p_i \rangle = p_i \tanh \left( \frac{p_i \cdot E}{3kT} \right). \quad (1)$$

The total polarization due to orientation of the dipole moments is equal to the sum of the contributions from individual regions. Thus, the static macroscopic polarization can be presented in the form

$$P(T, E) = \frac{1}{V_{cr}} \sum_{i=1}^{nr} \langle p_i \rangle + \epsilon_0 \epsilon_\infty E \quad (2)$$

where  $V_{cr}$  is the volume of the crystal,  $\epsilon_0$  is the dielectric permittivity of the vacuum and  $\langle p_i \rangle$  is given by (1).

The low-field static relative dielectric permittivity can be obtained from (2) as a derivative of  $P(T, E)$  with respect to the field at the limit  $E \rightarrow 0$ :

$$\epsilon_s = \frac{1}{3V_{cr}kT\epsilon_0} \sum_{i=1}^{nr} p_i^2 + \epsilon_\infty. \quad (3)$$

In the fast-changing electric field, when dielectric properties of relaxors are frequency dependent, each polar region behaves as an independent Debye-type relaxator with its relaxation time  $\tau$ . The reorientation of the local spontaneous polarization vector of a single region between equivalent states is considered to be a thermally activated process with an energy barrier between the stable states depending upon the anisotropy energy density,  $\Delta G_a$ , and the volume of the polar region, and equal to  $\Delta G_a l^3$ . A relaxation time is, therefore, given by

$$\tau = \tau_0 \exp \left( \frac{\Delta G_a l^3}{kT} \right). \quad (4)$$

From the LGD theory of ferroelectrics, the value of  $\Delta G_a$  depends upon the magnitude of the local spontaneous polarization,  $P_{s,i}$ , and the local transition temperature,  $T_{c,i}$ . At temperature  $T$  within the temperature range where the polar regions exist, a distribution of relaxation times in the relaxor stems from the distribution of transition temperatures: there coexist regions with long relaxation times (and high transition temperatures) and short ones (regions have appeared a few degrees above  $T$ ). The dielectric properties are represented as a superposition of individual relaxators, each of them giving the contribution depending upon its relaxation time. The complex relative dielectric permittivity  $\epsilon^*(\omega, T)$  can be found as

$$\epsilon^*(\omega, T) = \frac{1}{3V_{cr}kT\epsilon_0} \sum_{i=1}^{nr} \frac{p_i^2}{1 + i\omega\tau} + \epsilon_\infty \quad (5)$$

with a relaxation time  $\tau$  given by (4).

Here we should emphasize the difference between the present model and that of Smolensky and Isupov [3, 4]. In their model the sum of the contributions from the individual polar regions was also employed. However, the summation was performed only over the regions of which local  $T_c$  was equal to the temperature  $T$ . On the other hand, in the present model all the polar regions with  $T_c \geq T$  contribute to the dielectric response. Therefore, in the Smolensky and Isupov model the number of the polar regions,  $n_T$ , would represent the distribution function of the local transition temperatures, but here it corresponds to the cumulative distribution function. This difference will become clearer later, in the analysis of the experimental data.

The behaviour of the dielectric response of a relaxor, given by equations (2), (3) and (5), is controlled by the distribution of the local transition temperatures: the magnitudes of  $p_i$  and  $\tau$  are functions of  $T_{c,i}$ , and  $n_T$  depends upon the distribution of  $T_{c,i}$ . The dielectric permittivity  $\epsilon_\infty$  has been introduced as an average value for the crystal; however, it also depends on the distribution of  $T_{c,i}$ . In order to judge how accurate the hypothesis about the distribution of the local transition temperatures is we are going to compare the temperature and frequency dependence of the dielectric response predicted by the model, i.e. equations (2), (3) and (5), in a wide temperature range with that measured during the experiment. The required model parameters will be obtained from the analysis of the static dielectric response of PMN. An approach to data analysis will be given in the next section.

### 3. An approach to data analysis

Equations (1) and (2) describe the static dielectric response and assume that the polarization is a single-valued function of the applied field. They cannot be used in the case when the polarization is frequency dependent or hysteretic. Actually, in relaxors the onset of dielectric hysteresis in  $P(T, E)$  and frequency dependence of dielectric properties start to be observed at the same temperatures, around  $T_{\max}$ . Thus, to test the model we should analyse the electric field dependences of induced polarization at temperatures above  $T_{\max}$ .

However, equations (1) and (2) may not be applied in their present form to the analysis of experimental data, for we do not know anything about the distribution of the transition temperatures. Instead, at temperature  $T$  we suggest replacing the system consisting of  $n_T$  polar regions with different values of the dipole moments  $p_i$  by an ensemble of  $n_T$  identical polar regions with the same magnitude of the dipole moment  $p$ . The value of  $p$  is such that the macroscopic polarization is the same for both systems at a given temperature  $T$ :

$$P(T, E) = Np \tanh\left(\frac{p \cdot E}{3kT}\right) + \epsilon_0 \epsilon_\infty E. \quad (6)$$

Hereafter we shall call  $p$  the dipole moment of the polar regions in the sense that it is the same for all the regions. In (6) we introduce the concentration of the polar regions  $N$  as  $N = n_T/V_{\text{cr}}$ .

The suggested replacement of an ensemble of the polar regions brings about a certain error in  $P(T, E)$ , though we believe that the error is not large, since we are considering the static response. The dipole moment of each polar region is a slowly changing function of temperature, and, therefore, the distribution of the values of  $p_i$  at a given temperature  $T$ , originating from the distribution of  $T_{c,i}$ , is insignificant. In the case of the dynamic response one must take into account the relaxation times  $\tau$  of individual regions (4), which change exponentially with temperature. Thus, the distribution of the local transition temperatures will produce a broad distribution of  $\tau$ , which one cannot replace with an average single relaxation time. Still, we understand that even for the static response the

suggested replacement needs quantitative justification. To do so we should have information about the function describing the distribution of the local transition temperatures. For the moment this function is unknown, but we expect to obtain it from the analysis of the data. For the present we take (6) for granted and shall discuss the self-consistency of the approach later, in section 6. The number of polar regions,  $n_T$ , represents in the model the cumulative distribution function of the local transition temperatures. After the replacement of an ensemble of the polar regions the value of  $n_T$  (or the concentration  $N$ ) does not change. An analysis of the experimental data will yield the temperature dependence of  $N$ , from which we can find the distribution function of the local transition temperatures. Equation (6) is already more suitable for the analysis of experimental data. It contains three independent parameters— $N$ ,  $p$  and  $\varepsilon_\infty$ . They are all temperature dependent. The correct way, therefore, would be to fit equation (6) to the experimental data for electric field dependences of the induced polarization at a given temperature and find the values of  $N$ ,  $p$  and  $\varepsilon_\infty$ . However, with three parameters unambiguous fitting is not possible; the results are strongly dependent upon the method of fitting.

To reduce the number of fitting parameters we introduce experimental data concerning the temperature dependence of the low-field static dielectric permittivity,  $\varepsilon'_s$ , of PMN. From equation (6)  $\varepsilon'_s$  can be obtained as

$$\varepsilon'_s = \frac{Np^2}{3kT\varepsilon_0} + \varepsilon'_\infty. \quad (7)$$

It is similar to the expression for static dielectric permittivity which is usually applied to describe the orientation polarization of polar dielectrics [13]. Let us assume that in the low-field limit this formula is also valid in the case of the orientation polarization of an ensemble of the polar regions. By using this assumption, we can combine equations (6) and (7) in the form

$$\varepsilon_s \varepsilon_0 E - P = Np \left( \frac{p \cdot E}{3kT} - \tanh \left( \frac{p \cdot E}{3kT} \right) \right) \quad (8)$$

where only two parameters,  $p$  and  $N$ , are involved.

To summarize, in order to analyse the polarization response of PMN in terms of the proposed model we shall use equation (8). For that we need to know the induced polarization  $P$  as a function of the applied field and the value of the low-field static dielectric permittivity  $\varepsilon'_s$ .

#### 4. Experimental details

Single-phase PMN powder was produced according to the method of Butcher and Daghli [14]. Pressed pellets were sintered at 1225 °C for 2 hours using a PMN atmosphere powder. The density of the sintered samples was about 98% of the theoretical. Gold electrodes were sputter deposited on the polished surfaces of the pellets.

The induced polarization of PMN ceramics as a function of the applied electric field was measured using a virtual Sawyer–Tower circuit at different temperatures within the range from 133 K to 393 K at 10 K intervals. The highest frequency in these measurements was equal to 25 Hz and the lowest one to 0.1 Hz. Measurements were performed for two amplitudes of the applied field  $E_m$ . An amplitude of 35 kV cm<sup>-1</sup> was applied in order to obtain saturated polarization curves at fields as high as possible for the given ceramic sample before dielectric breakdown would occur. At the same temperatures, polarization was measured at  $E_m = 1$  kV cm<sup>-1</sup> in order to calculate the relative dielectric permittivity in

the low-field limit. The amplitude of the applied field of  $1 \text{ kV cm}^{-1}$  was the lowest value imposed by the equipment and dimensions of the sample. The waveform of the applied field was triangular.

The real and imaginary parts of the dielectric permittivity were measured using a HP 4284 A LCR meter, over five decades of frequency (20 Hz–1 MHz), and over the temperature range 170–450 K. These ‘standard’ dielectric measurements are for the purpose of comparison of the temperature and frequency behaviour of the low-field permittivity calculated from the model with that observed in the experiment.

Temperature control in both experiments was maintained with a Delta Design 9023 temperature chamber.

The electric field dependences of the induced polarization measured at  $35 \text{ kV cm}^{-1}$  are shown in figures 1(a) and 1(b) for several temperatures, and are similar to those reported in the literature [1, 2]. At low temperatures rather rectangular dielectric hysteresis loops are observed. With an increase in temperature loops become tilted, having values of remanent polarization and coercive field which decrease with increasing temperature. At higher temperatures dielectric hysteresis disappears, and polarization is a single-valued function of the applied field. The polarization plotted against the field has the shape of a non-linear curve with a saturation reached in high field. With increasing temperature the magnitude of the electric field needed to reach the saturation becomes higher (figure 1(b)). At high temperatures, at 373 K in figure 1(b), the saturation is not observed at  $35 \text{ kV cm}^{-1}$ ; however, the non-linearity of the polarization is still noticeable.

The electric field dependences of the induced polarization measured at  $E_m = 1 \text{ kV cm}^{-1}$  at low temperatures have the shape of an ellipse and at higher temperatures become a straight line. The values of  $\epsilon'$  and  $\epsilon''$  calculated from the low-field polarization data (at high temperatures  $\epsilon'' = 0$  within experimental error and  $\epsilon'$  is equal to the slope of a straight line) are in good agreement with those which have been measured with conventional techniques.

In PMN the temperature at which dielectric hysteresis appears on cooling depends upon the measurement frequency. For the lowest frequency used in these experiments the ‘onset’ temperature is between 243 and 253 K.

## 5. Analysis of the experimental data within the model

For the lowest frequency used in the polarization measurements, 0.1 Hz, dielectric hysteresis is observed at temperatures below 250 K. Therefore, at temperatures above 250 K we can take values of the induced polarization and relative permittivity measured at 0.1 Hz as static ones and use them in equation (8) as  $P(T, \mathbf{E})$  and  $\epsilon'_s$  respectively. At every temperature above 250 K the experimental data for the permittivity and  $P(T, \mathbf{E})$  have been modified in the form  $\epsilon_s \epsilon_0 \mathbf{E} - \mathbf{P}$  and fitted to equation (8) using  $N$  and  $p$  as parameters. The experimental electric field dependences of the polarization at each temperature were first smoothed using a locally weighted least-squares error method. This was done in order to reduce the scatter of the data, because even a very small experimental error,  $\Delta P$ , which is insignificant in comparison to the total value of measured polarization, becomes very important for the function  $\epsilon_s \epsilon_0 \mathbf{E} - \mathbf{P}$ , especially at high temperatures. Such a scatter in the data may produce a large uncertainty in results of the fitting with (8). The results have shown that the fit of the experimental data to equation (8) with only two parameters is unique.

When the parameters  $N$  and  $p$  are known, one can calculate saturation polarization,  $P_{\text{sat}}$ , when all the dipole moments are parallel to the external field, the size  $L$  of the volume of the crystal containing a single polar region,  $\epsilon'_p$  which is a contribution from the orientation of



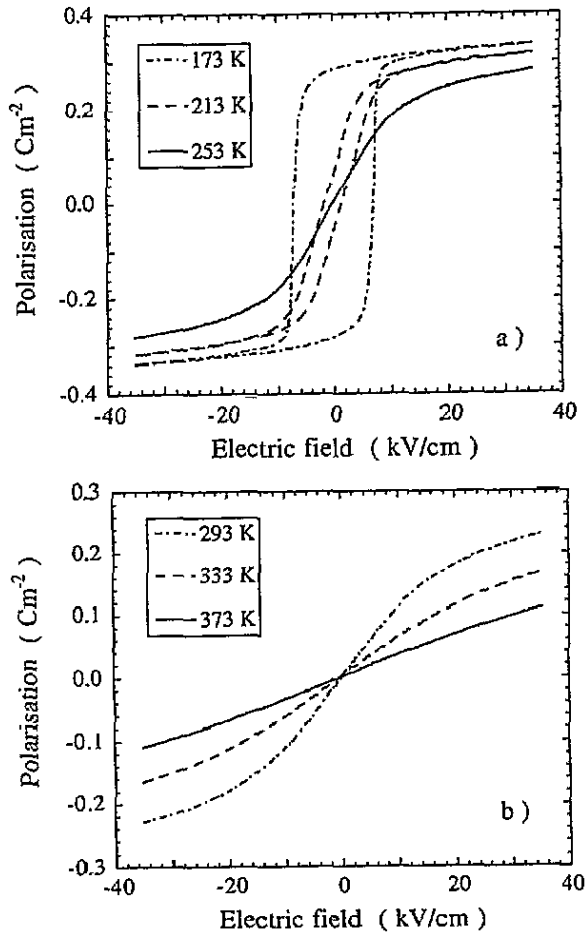


Figure 1. Induced polarization of PMN ceramics as a function of the applied electric field at several temperatures (the frequency is 0.1 Hz, for which the temperature of the dielectric permittivity maximum is about 250 K).

the dipole moments to the dielectric permittivity of the crystal and high-frequency dielectric permittivity  $\epsilon_{\infty}$ , by using the following formulae:

$$P_{\text{sat}} = Np \quad (9a)$$

$$L = N^{-1/3} \quad (9b)$$

$$\epsilon_p = \frac{Np^2}{3kT\epsilon_0} \quad (9c)$$

$$\epsilon_{\infty} = \epsilon_s - \epsilon_p \quad (9d)$$

where  $\epsilon'_s$  is the static permittivity measured in the experiment.

The dipole moment of the polar regions (figure 2) and the concentration of the polar regions in the crystal (figure 3) increase with decreasing temperature. Their temperature dependences within the temperature range addressed may be described rather well by a linear function. The saturation polarization as a function of temperature is shown in figure 4 in comparison with the polarization measured at  $35 \text{ kV cm}^{-1}$ . The magnitude of  $P_{\text{sat}}$  tends

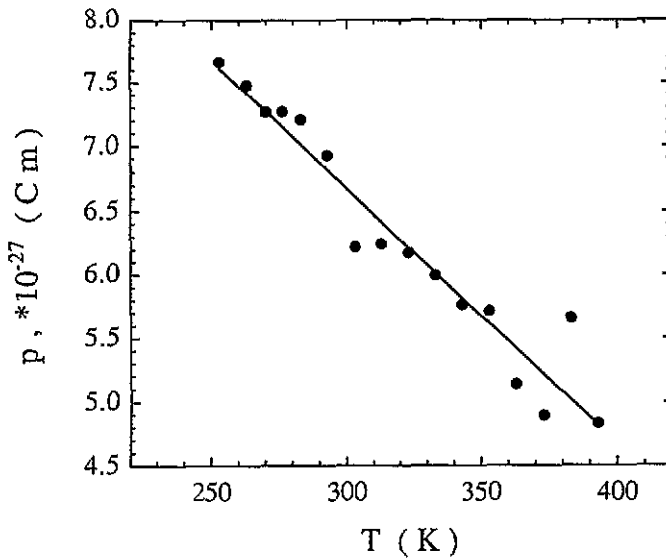


Figure 2. Dipole moment  $p$  of an ensemble of the identical polar regions for PMN ceramics (the line is the fit with a linear function).

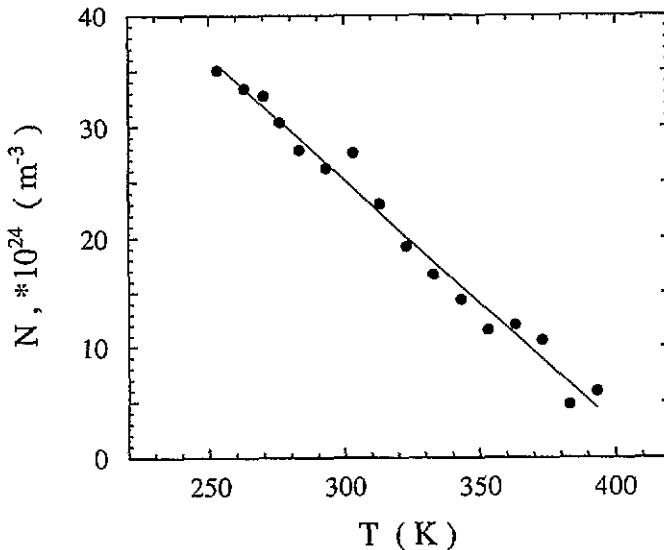


Figure 3. Concentration of the polar regions as a function of temperature for PMN ceramics (the line is the fit with a linear function).

to zero at temperatures above 410 K. On cooling, the saturation polarization increases and, at temperatures around 250 K, it becomes very close to the magnitude of the polarization measured at 35 kV cm<sup>-1</sup>. Dielectric permittivity  $\epsilon'_p$  due to the orientation of the dipole moments is not shown here; it drastically increases in the range from 370 K to 250 K as a result of increase in  $p$  and  $N$  with decreasing temperature  $T$ . At high temperatures, approximately above 410 K,  $\epsilon'_p \rightarrow 0$ . The high-frequency dielectric permittivity,  $\epsilon_\infty$ , was calculated with (9d) and its temperature dependence is shown in figure 5. On cooling,  $\epsilon_\infty$  goes through the maximum value at temperatures around 350 K. Above 410 K, where

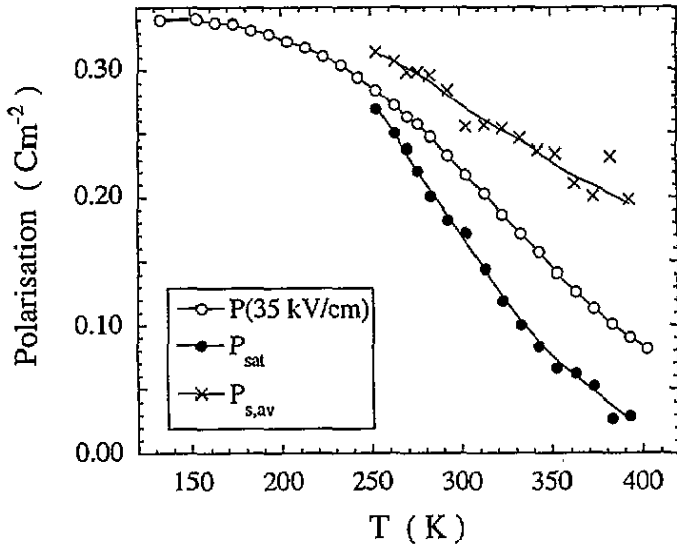


Figure 4. Temperature dependence of the polarization measured at  $35 \text{ kV cm}^{-1}$ , saturation polarization due to orientation of the dipole moments of the polar regions and the polarization  $P_{s,av}$  (the lines are to guide the eyes).

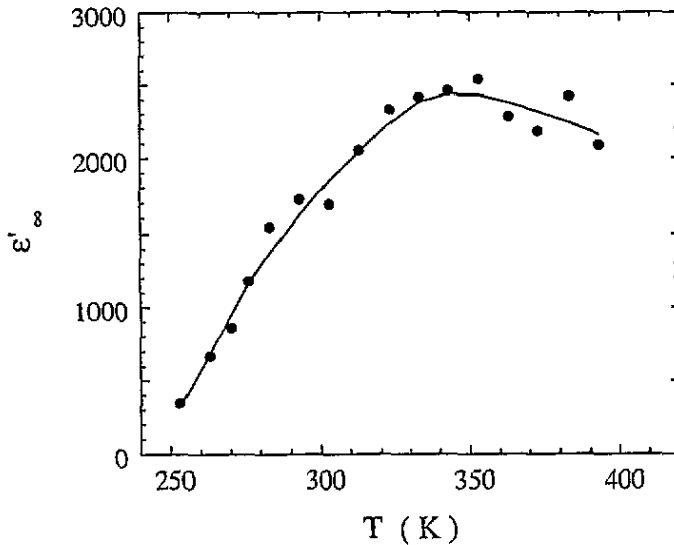


Figure 5. High-frequency relative dielectric permittivity  $\epsilon'_{\infty}$  of PMN (the line is drawn to guide the eyes).

$\epsilon'_p \approx 0$ , the measured dielectric permittivity coincides with  $\epsilon_{\infty}$ .

In order to estimate the quality of the fitting of the experimental data to equation (8) we used the obtained values of  $p$ ,  $N$  and  $\epsilon_{\infty}$  to calculate a total polarization response with equation (6) and compare it with the experimental data on  $P(T, E)$ . At every temperature from the range above 250 K there was a very good agreement between the experimental values of the polarization and those calculated from the obtained parameters of the model. For example, figure 6 shows both measured and calculated polarization curves at 293 K.

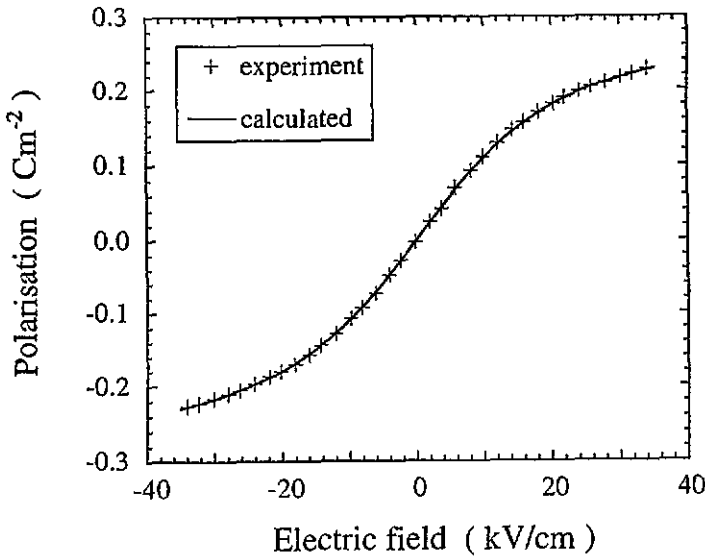


Figure 6. Polarization as a function of the applied electric field of PMN ceramics at 293 K: measured and calculated from the obtained values of  $p$ ,  $N$  and  $\epsilon'_{\infty}$ .

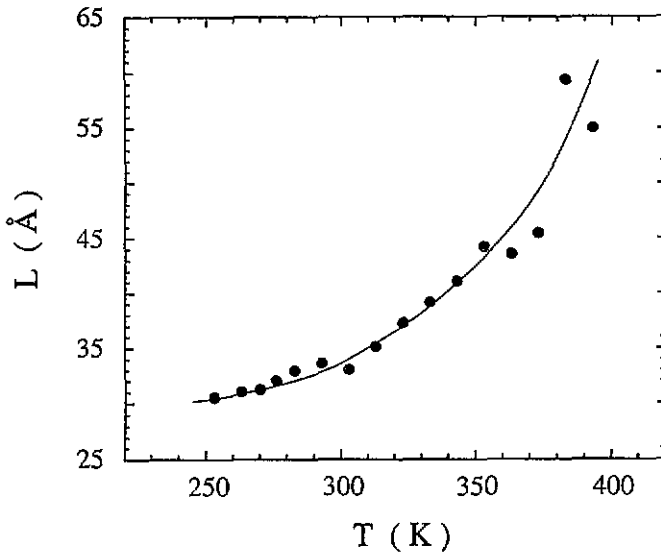


Figure 7. Temperature dependence of the size of the crystal volume containing single polar region for PMN (the line is to guide the eyes).

The size of the volume of the crystal containing a single polar region,  $L$ , is shown in figure 7. It decreases on cooling, and at low temperatures it tends to a value of  $\sim 30\text{\AA}$ . The temperature dependence of  $L$  corresponds to that of the concentration of the polar regions in the crystal. As the total number of regions increases (figure 3), the volume of the crystal containing a single polar region must be smaller. If we assume that the size of an individual polar region,  $l$ , does not change with temperature, we can estimate it as a low-temperature limit of  $L$ . From figure 7 one can see that  $L$  does not change significantly below 260 K. By extrapolating the temperature dependence of  $L$  down to low temperatures we can estimate

the size of the polar regions as being equal to 30 Å. The value of  $l$  obtained in this way is in good agreement with the estimate of the size of the polar regions suggested by a structural study of PMN and equal to 100 Å [12].

Now, when the value of the size of the regions is known, we can find an average local spontaneous polarization corresponding to the dipole moment  $p$  by  $P_{s,av} = p/l^3$ . The temperature dependence of  $P_{s,av}$ , is shown in figure 4.

The concentration of the polar regions  $N$  as a function of temperature represents the distribution of local transition temperatures. Just above we discussed the fact that the size of the volume of the crystal containing a single polar region at low temperatures, below 250 K, tends to the limit value equal to the size of the polar region. This actually means that at low temperatures the concentration of the polar regions reaches its saturation value and the whole volume of the crystal is occupied by the polar regions. Therefore, within the temperature range 250 K to 390 K we can normalize the concentration  $N$  to its saturation value, which is equal to  $l^{-3} \approx (30\text{Å})^{-3}$ , and introduce a cumulative distribution function of the transition temperatures  $Y$  as

$$Y = N(30 \text{ Å})^3. \quad (10)$$

Following Smolensky and Isupov [3] we assume that the distribution of local transition temperatures is given by a Gaussian function around a mean value of the Curie temperature,  $T_{c,m}$ , with a width of distribution  $\sigma_T$

$$y(T_c) = \frac{1}{\sqrt{2\pi}\sigma_T} \exp\left(-\frac{(T_c - T_{c,m})^2}{2\sigma_T^2}\right). \quad (11)$$

In this case a cumulative distribution function is described by the error function:

$$\text{erf}(T) = \int_T^\infty y(T_c) dT_c.$$

A good fit of  $Y$  to  $\text{erf}(T)$  was obtained for the following parameters: the mean transition temperature  $T_{c,m} \approx 320$  K and  $\sigma_T \approx 60$  K. Figure 8 shows the result of the fitting.

Before finishing this section we can make preliminary conclusions about the change in the magnitude of the two contributions to the polarization response, the high-frequency and orientation polarizations. At high temperatures (about 370 K) the polarization is due to the response of crystal lattice rather than orientation of the dipole moments of the polar regions. On cooling the contribution from the orientation polarization increases, and around 250 K it becomes dominant over the response of the crystal lattice. The reason for this is that the magnitude of the dipole moment  $p$  and the concentration  $N$  of the polar regions both increase with decreasing temperature. The latter, however, plays the more important role in this process. This can be concluded from the comparison of the temperature dependences of  $P_{sat}$  and  $P_{s,av}$  plotted in figure 4. Within the studied temperature range, 250 K to 390 K,  $P_{s,av}$  does not change significantly, whereas  $P_{sat}$  drastically drops to very small values at temperatures around 390 K. At the same time at high temperatures  $P_{s,av}$  has a rather high value of about  $0.20 \text{ C m}^{-2}$ . Therefore, it is the concentration of the polar regions which enters the formula for the saturation polarization (9a) and accounts for its drastic decrease at high temperatures.

## 6. The dielectric response of relaxors calculated from the model

In the previous section we analysed the static dielectric response of PMN in order to obtain the model parameters as a function of temperature. Here we shall present a way of calculating

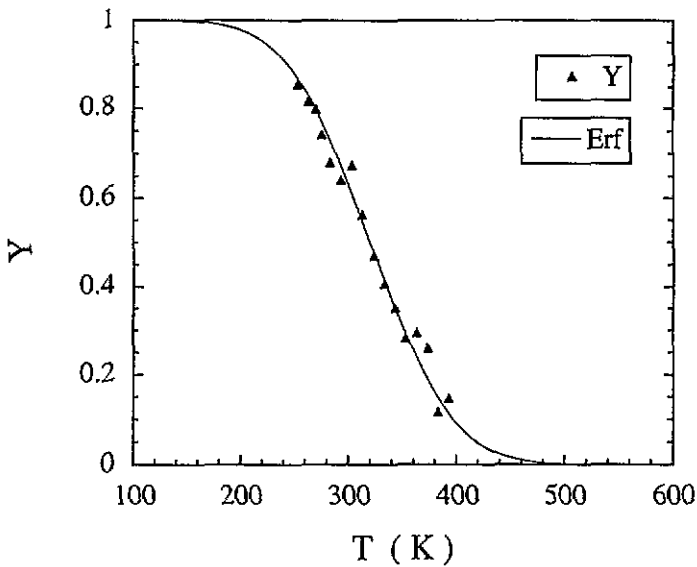


Figure 8. Cumulative distribution function  $Y$  of local transition temperatures and its fit using the error function erf. Mean transition temperature  $T_{c,m} = 320$  K and  $\sigma_T = 60$  K.

the dielectric response of relaxors, both static and dynamic, in terms of the model introduced in section 2. We shall consider only the polarization due to orientation of the dipole moments of the polar regions. We do not take into account the high-frequency response,  $\epsilon'_{\infty}$ , although it also can be modelled. We shall also present the verification of the validity of the approach which we described in section 3 and used in the analysis of the experimental data.

Still working within the model described in section 2 we use three basic assumptions

(a) We consider a relaxor as an ensemble of non-interacting polar regions. Each region is an independent, normal ferroelectric with the low-temperature phase with a rhombohedral symmetry. The magnitude of a local spontaneous polarization  $P_s$  of individual regions depends upon the local transition temperature  $T_c$  and the temperature  $T$  of the crystal and may be found in terms of the LGD theory of ferroelectrics.

(b) The distribution of local transition temperatures of individual regions is described by a Gaussian function (11) with the values of the parameters taken from the results presented in the previous section. They are equal to  $T_{c,m} = 320$  K and  $\sigma_T = 60$  K.

(c) All the regions have the same size  $l$  equal to  $30 \text{ \AA}$ .

### 6.1. Dielectric response

In previous sections it was convenient to use in all the expressions the dipole moment of the polar regions. Now, since we are trying to simulate the polarization response by using the LGD formalism for ferroelectrics, and the size of the polar region is known, it is more convenient to work in terms of the local spontaneous polarization,  $P_s$ . The contribution from individual regions to the orientation polarization is determined by the magnitude of the local spontaneous polarization  $P_s$ , which, in turn, is directly related to the value of the local transition temperature. At a given temperature  $T$ , only the regions with  $T_c$  greater than  $T$  contribute to the orientation polarization.

To perform the calculations we suggest modifying equations (2), (3) and (5), to write them in terms of the distribution function  $y(T_c)$ . It is straightforward to show that the static

polarization, static permittivity and complex dielectric permittivity due to the orientation of the dipole moments of the polar regions may be written, respectively, as (we omit only the high-frequency response given by  $\epsilon'_{\infty}$ )

$$P(T, E) = \int_T^{\infty} y(T_c) P_s \tanh\left(\frac{P_s \cdot l^3 E}{3kT}\right) dT_c \quad (12)$$

$$\epsilon'_s = \frac{l^3}{3kT\epsilon_0} \int_T^{\infty} y(T_c) P_s^2 dT_c \quad (13)$$

$$\epsilon^*(\omega, T) = \frac{l^3}{3kT\epsilon_0} \int_T^{\infty} \frac{y(T_c) P_s^2}{1 + i\omega\tau} dT_c \quad (14)$$

where  $P_s$  is a function of  $T_c$  and  $T$ , and the relaxation time  $\tau$  is given by (4).

### 6.2. Relaxation time spectrum

At temperatures approximately below that of the relative dielectric permittivity maximum relaxors display relaxation behaviour of the dielectric permittivity within the radiofrequency range. It was shown by a number of authors, Dorogovtsev and Yushin [9], Viehland *et al* [10] and Colla *et al* [11], that the relaxation is distinctly non-Debye. The dielectric response of relaxors is governed by an ensemble of relaxators with a broad spectrum of relaxation times. On cooling the width of the spectrum increases.

In terms of the model discussed here, a distribution of relaxation times in the relaxor stems from the distribution of Curie temperatures. We introduce the function  $g(z, T)$ , where  $z = \ln \tau/\tau_0$ , describing the distribution of relaxation times at temperature  $T$ . The total number of relaxators in the system is represented by the value of  $Y(T)$ :

$$Y(T) = \int_T^{\infty} y(T_c) dT_c. \quad (15)$$

Amongst them the number of relaxators with relaxation times given by  $z$ , within the interval  $z$  to  $z + dz$ , is equal to  $Y(T)g(z, T)dz$ . Since the difference in the values of  $z$  is accounted for by the difference in the transition temperatures  $T_c$ , the same number of relaxators will be equal to  $y(T_c) dT_c$ . Therefore, we can find the value of  $g(z, T)$  from

$$g(z, T) = \frac{y(T_c(z)) dT_c}{Y(T) dz} \quad (16)$$

The relationship between  $T_c$  and  $z$  may be obtained from the formula

$$z = \frac{\Delta G_a(T_c) l^3}{kT} \quad (17)$$

which is a direct consequence of equation (4) for relaxation time  $\tau$ .

### 6.3. Quantitative estimation of the validity of the approach introduced in section 3

In section 3 in order to make possible the analysis of the experimental data we replaced an ensemble of different regions by a system of identical ones and afterwards used equation (6) instead of (2). At that time we could not give any quantitative justification for doing so. The main reason was that we did not have any information about the distribution of the values of the dipole moments at temperature  $T$ . Now we know that function  $y(T_c)$  describing the distribution of the local transition temperatures is given by (11). Therefore it

would be useful to derive an equation similar to (6) by using the expression for  $y(T_c)$  and try to estimate quantitatively the error which is introduced by such a replacement. All the mathematical details of this can be found in the appendix. Here we mention only that in terms of the local transition temperatures, replacement of an ensemble of different regions by a system of identical ones means that we replace the distribution of  $T_c$  (for  $T_c > T$ ) by a single temperature  $T^*$  corresponding to the value of the local spontaneous polarization of identical polar regions. Mathematically, the function  $y(T_c)$ , at  $T_c > T$ , is replaced by the delta function  $\delta(T_c - T^*)$ . This is illustrated in figure 9. It is straightforward to obtain from (12) the following expression for the orientation polarization:

$$P(T, E) = Y(T)P_s(T, T^*) \tanh \left( \frac{P_s(T, T^*) \cdot l^3 E}{3kT} \right). \tag{18}$$

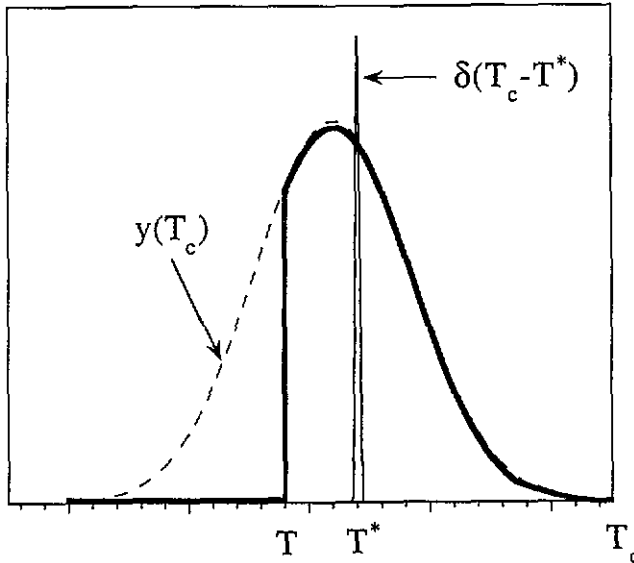


Figure 9. Distribution function  $y(T_c)$  of the local transition temperatures, part of  $y(T_c)$  showing that only regions with  $T_c > T$  contribute to the orientation polarization (drawn by bold solid line) and delta function  $\delta(T_c - T^*)$ .

It is clear that equation (18) is equivalent to (6) to within  $\epsilon'_{\infty}$ . The suggested replacement of an ensemble of the polar regions introduces an error in  $P(T, E)$ , the value of which depends upon the magnitude of the electric field,  $E$ . However, the replacement can be done exactly at low-field limit. Assuming that the applied field  $E$  is low enough we can derive from (12) and (18) the following relationship:

$$P_s^2(T, T^*) = \frac{1}{Y(T)} \int_T^{\infty} y(T_c) P_s^2(T, T_c) dT_c \tag{19}$$

which permits us to find  $T^*$ . Thus, our approach is to calculate  $T^*$  from (19) and then evaluate the errors introduced in  $P(T, E)$  by such a replacement. Before finishing this section it must be noted that we should not expect that  $T^*$  remains the same for all temperatures  $T$  where the polar regions exist, because of the way in which we introduced it.



### 7. Simulation of dielectric properties of relaxors for the model ferroelectric

In this section we present the results of simulation of the dielectric response of relaxors. The results of the analysis of static dielectric response of PMN, which have been presented in section 5, allow us to perform the calculations over the wider temperature range, and consider the frequency dependence of the dielectric properties of relaxors. Here we assume that the polar regions behave as a model ferroelectric with second order phase transition with well known free energy coefficients. For the second-order phase transition the calculations are rather simple. The results of simulations will be compared with those obtained from the experimental data for PMN. The comparison can be done here only qualitatively, since the free energy coefficients of the chosen materials do not necessary coincide with those for PMN (which are not known).

The elastic Gibbs energy of a ferroelectric with a rhombohedral structure, with reference to the unpolarized state, is expressed in terms of a Taylor series expansion in spontaneous polarization  $P_s$ . For simplicity, the series is terminated here at the fourth power of  $P_s$ :

$$\Delta G_1 = -\alpha_1(T_c - T)P_s^2 + \frac{(\alpha_{11} + \alpha_{12})}{3}P_s^4. \quad (20)$$

Spontaneous polarization depends upon the temperature as

$$P_s^2 = \frac{3\alpha_1(T_c - T)}{2(\alpha_{11} + \alpha_{12})}. \quad (21)$$

The anisotropy energy density as a function of temperature is given by

$$\Delta G_a = \frac{3\alpha_1^2(T_c - T)^2}{4(\alpha_{11} + \alpha_{12})}. \quad (22)$$

As a model ferroelectric we have chosen  $\text{Pb}(\text{Zr}_{0.6}\text{Ti}_{0.4})\text{O}_3$ , which is a perovskite with a second-order ferroelectric phase transition and a rhombohedral polar phase. The values of its free energy coefficients are known and given by Haun *et al* [15]. They are equal to

$$\alpha_1 = 2.330 \times 10^5 \text{ m F}^{-1} \text{ K}^{-1}$$

$$\alpha_{11} = 1.362 \times 10^8 \text{ m}^5 \text{ C}^{-2} \text{ F}^{-1}$$

$$\alpha_{12} = 2.391 \times 10^8 \text{ m}^5 \text{ C}^{-2} \text{ F}^{-1}.$$

Calculations have been performed for  $T$  from the temperature range 100 K to 450 K. Every time, when it was necessary to integrate over the distribution of the transition temperatures, for the upper integration limit we chose  $T_{c,m}$  plus three times the width of the distribution of the transition temperatures, since beyond this limit the contributions to corresponding integrals were negligible.

The results of calculations of  $T^*$  with (19) have shown that it changes with the temperature  $T$  of the sample in the following way. When  $T > 300$  K temperature  $T^*$  increases with  $T$ , being always several tens of degrees higher than  $T$ . Below 300 K  $T^*$  changes slowly, and below 200 K it stays constant and equal to 320 K (that is, to the mean transition temperature  $T_{c,m}$ ). The maximum values of the errors introduced in  $P(T, E)$  by the replacement of an ensemble of the polar regions have been estimated from equations (A14) given in the Appendix. They are smaller than 10% in the temperature range from 140 K to 420 K. Thus, they are low enough to be neglected (at least, within the temperature range 250 K to 400 K, where we studied polarization response). We can draw the following conclusions. For the model of relaxor behaviour presented in section 2 the substitution of an ensemble of the polar regions with different values of the dipole moment by a system of

identical polar regions with the same magnitude of the dipole moment does not introduce large errors. Such a replacement does not contradict the original assumption that all the polar regions have different dipole moments; however, it aids in the analysis of experimental data.

The static dielectric response was calculated from the formulae (12) and (13). The static dielectric permittivity,  $\epsilon'_s$ , increases monotonically with decreasing temperature, the behaviour being mostly determined by the factor  $T^{-1}$  in (13). The integral

$$\int_T^\infty y(T_c) P_s^2 dT_c$$

in the same formula is less significant. Static polarization calculated with (12) as a function of the applied field at the fixed temperature has the shape of a non-linear curve and resembles well the experimental  $P(E)$  data, which are shown, for example, in figure 1(b). It is interesting to demonstrate the change in the orientation polarization with temperature at a fixed value of the applied field. The value of the field of  $35 \text{ kV cm}^{-1}$  was chosen and the polarization at this field was calculated as a function of temperature. We compare the model and experimental values of the polarization at  $35 \text{ kV cm}^{-1}$  in figure 10. Points denoted as experimental were obtained from the measured values of the polarization by subtracting the high-frequency contribution represented by  $\epsilon'_\infty$ . For the most part the model qualitatively corresponds well to the experiment. However, at low temperatures ( $\leq 250 \text{ K}$ ) the experimental values reach saturation, but the model ones still continue to grow. This difference may be a sign that at low temperatures the properties of the material probably undergo transformations which are not accounted for by the model.

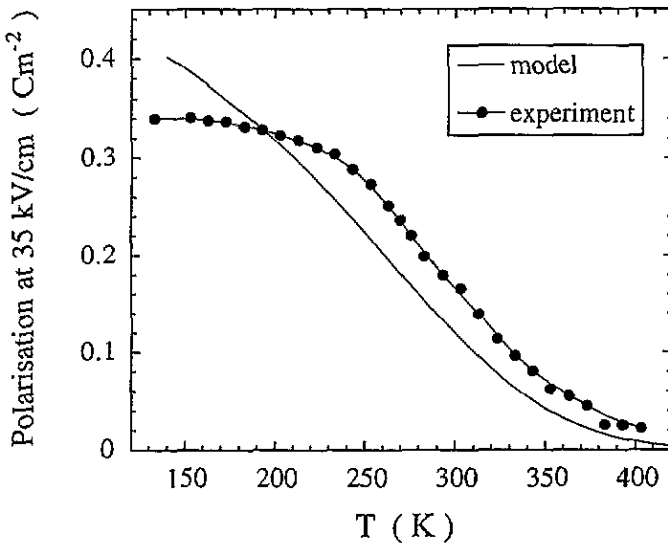


Figure 10. The static orientation polarization at  $35 \text{ kV cm}^{-1}$  calculated from the model and obtained from the experimental data for PMN.

The complex dielectric permittivity was modelled by using equation (14). The value of parameter  $\tau_0$ , which enters the formula (4) for the relaxation time, was estimated as  $2 \times 10^{-13} \text{ s}$  (it is inversely proportional to the magnitude of the typical frequency of optical phonons). The real part of the dielectric permittivity as a function of temperature is plotted in figure 11(a) for several frequencies. The static permittivity is shown in the same figure for

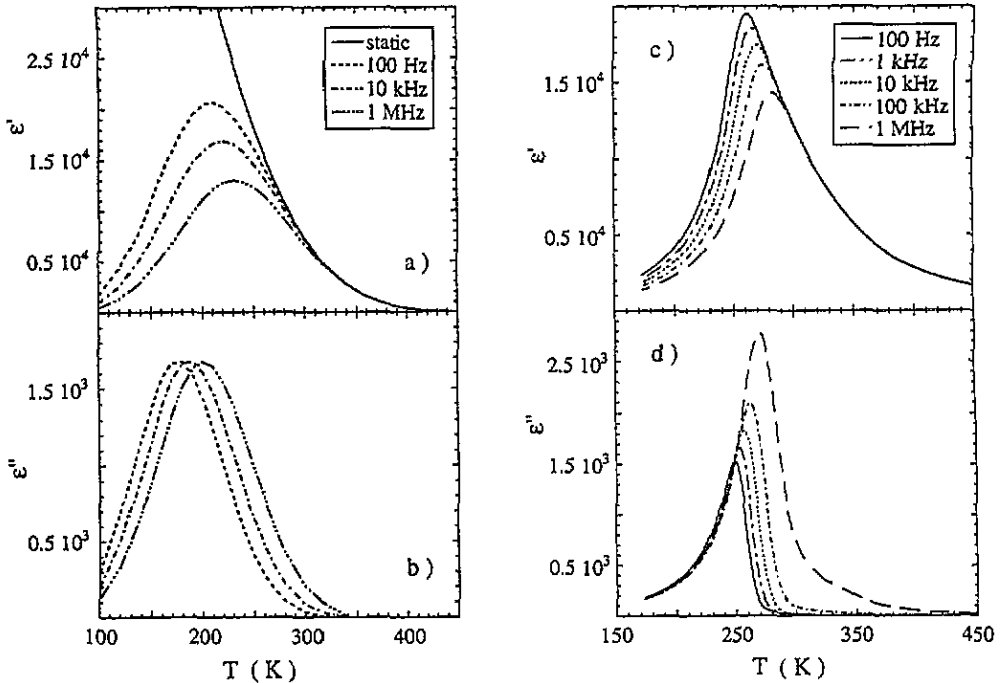
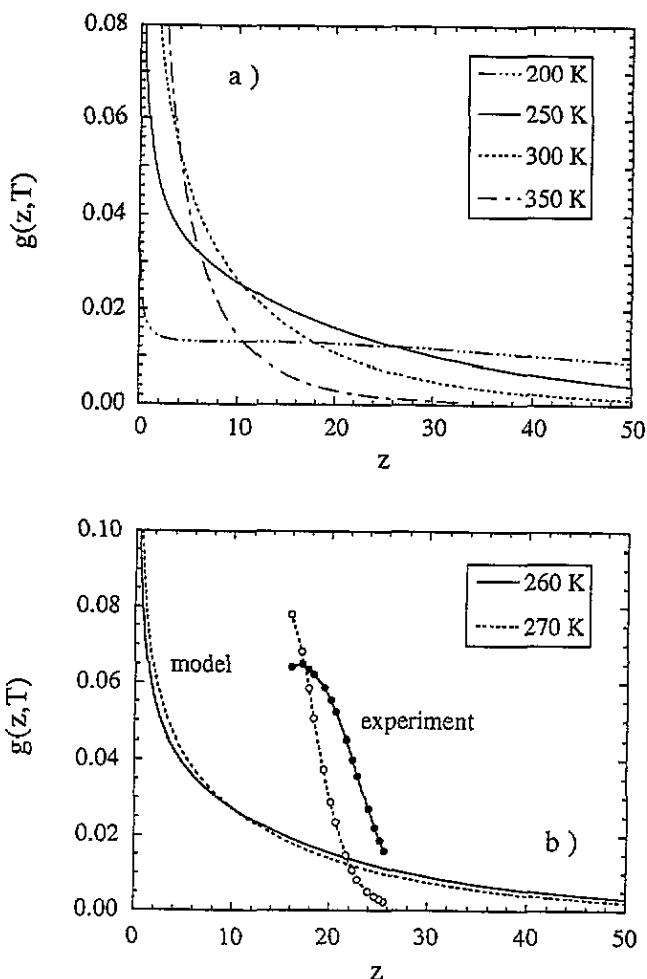


Figure 11. Real ( $\epsilon'$ ) and imaginary ( $\epsilon''$ ) parts of the dielectric permittivity as a function of temperature at several frequencies: (a) and (b), calculated from the model (the real part is given in comparison with the static dielectric permittivity); (c) and (d), measured in the experiment.

comparison. At high temperatures the relative permittivity coincides with the static one at every frequency. On cooling,  $\epsilon'(\omega, T)$  at first deviates from  $\epsilon'_s(T)$ , then it passes through a maximum and at low temperatures decreases to very small values. This actually means that at low temperatures the majority of relaxators have relaxation times which are too long to respond to the external electric field on a laboratory time scale. They appear 'blocked' in one of the states. The imaginary part of the relative permittivity also passes through a maximum on cooling (figure 11(b)). With increasing frequency the curve  $\epsilon''(\omega, T)$  shifts to higher temperature without a change in the magnitude of the maximum value. The relaxation time spectrum calculated with (16) is shown in figure 12(a) for several temperatures. It broadens with decreasing temperature and the maximum relaxation time in the spectrum (which corresponds to largest  $z$ ) tends to a very large value.

To summarize, simulations have shown the effect of the slowing down of fluctuations of the dipole moments of the polar regions on the dynamic dielectric properties of PMN. This slowing down occurs as a consequence of increasing local polarization and decreasing thermal energy of the crystal. It may qualitatively account for the behaviour of dielectric permittivity which is usually observed in the experiment.

One can compare the behaviour of real and imaginary parts of dielectric permittivities calculated according to the model (figures 11(a), (b)) with those measured in the experiment (figures 11(c), (d)) and find certain discrepancies between the model and experimental data. It is easy to explain the difference in the behaviour of  $\epsilon'(\omega, T)$  at high temperatures, above  $\sim 350$  K. It could be attributed to the fact that model describes only orientation polarization and does not take into account the high-frequency response. That is why in this model the real part of the dielectric permittivity tends to zero at temperatures around 450 K.



**Figure 12.** Relaxation time spectrum for PMN at several temperatures: calculated in terms of the model (a) and given in comparison with the spectrum obtained from the experimental data (b);  $z = \ln(\tau/\tau_0)$ .

Perhaps the most serious discrepancy between the model and the experiment can be found in the properties related to the relaxation time spectrum. One can obtain the function  $g(z, T)$  from the experimental data by using the following approach (see [9] and [11], for example). If the relaxation time spectrum is smooth and wide enough it can be calculated from the imaginary part of the dielectric permittivity measured at different frequencies at temperature  $T$  as

$$g(z, T) = \frac{2}{\pi} \frac{\varepsilon''(z, T)}{\varepsilon'_s(T)} \quad (23)$$

where  $\varepsilon'_s(T)$  is the static dielectric permittivity at temperature  $T$ , and the magnitude of  $z$  is calculated as  $z = \ln(1/\omega\tau_0)$  with  $\omega$  as measurement frequency and  $\tau_0 = 2 \times 10^{-13}$  s. Assuming that the condition of smoothness and broadness of the spectrum is fulfilled for relaxors, Colla *et al* [11] have shown that for the PMN spectrum in a wide temperature range has the shape of a broad regular function with a maximum, and tending to zero

values at both long and short relaxation times. Taking the data on the low-field dielectric permittivity we calculated the values of the function  $g(z, T)$  with equation (23) at two temperatures and plotted them in figure 12(b) (drawn by lines with circles). The spectrum calculated from the model is shown in the same plot (drawn by lines only). The interval of  $z$  within which experimental curves are plotted is limited by the frequency range used in the experiment—20 Hz to 1 MHz. At two selected temperatures experimental curves represent only a long-relaxation-time tail of the spectrum. It is seen that spectrum has a rather abrupt edge at long relaxation times. In contrast, in the model the function  $g(z)$  tends to zero gradually when  $z \rightarrow \infty$ . The properties of the spectrum at long relaxation times may explain the difference in the behaviour of  $\epsilon'(\omega, T)$  at temperatures where it deviates from the  $\epsilon'_s(T)$ —around 300 K in figure 11(a) (model) and 250–300 K in figure 11c (experiment). An apparent 'cut-off' in the relaxation time spectrum, at around  $z = 25$  (figure 12(b)), makes it possible to specify the frequency range where the dielectric permittivity will display relaxation behaviour and where it will be frequency independent. However, in the case of a gradual decrease of  $g(z)$ , as predicted by the model, frequency dispersion would be observed in the whole frequency range below  $1/\tau_0$ .

It seems also that the properties of the short-relaxation-time limit of the spectrum ( $z \approx 0$ ) are different in the model and what is observed in practice. It has been already mentioned that Colla *et al* [11] have shown that for PMN,  $g(z) \rightarrow 0$  as  $z \rightarrow 0$  in a wide temperature range. From the model applied for the ferroelectric with second-order phase transition it follows that the function  $g(z, T)$  diverges at  $z \rightarrow 0$  as  $1/\sqrt{z}$  for every temperature involved in simulations (this is seen from equations (17) and (22)). The divergence of  $g(z, T)$  directly follows from the model; however, its meaning is not clear. The important thing is that the number of relaxators having values of  $z$  within the limited interval is equal to

$$\int_0^z g(z, T) dz$$

and does not diverge as  $z \rightarrow 0$ .

## 8. Discussion

Crystalline disorder, which is a common characteristic of relaxors, may cause the distribution both of the local transition temperatures of the polar regions and their sizes. In previous papers [7, 8] the effect of the distribution of the size of the polar regions on the dielectric properties of relaxors has been demonstrated. Here we attempted to investigate the second possibility, the distribution of the local transition temperatures.

The model presented in this paper considered a relaxor as an ensemble of non-interacting polar regions, the dipole moments of which can be oriented by the external electric field. As a first test for the model we tried to fit it to experimentally measured static polarization of PMN as a function of the electric field and temperature. Using only one assumption, that the number of the polar regions is temperature dependent, the change of the static polarization of PMN was described in a temperature interval of 150 K, and electric field up to 35 kV cm<sup>-1</sup>.

However, to find the size of the polar regions, and the distribution function of the local transition temperatures, an additional assumption, that all the polar regions have the same size,  $l$ , was required. The value of  $l$  was estimated as a low-temperature limit of the size of the crystal volume containing a single polar region plotted in figure 7. It was found to be equal to 30 Å, in good agreement with the estimate suggested by structural study of PMN and equal to 100 Å [12]. The distribution function of the local transition temperatures,

$y(T_c)$ , was calculated from the temperature dependence of the concentration of the polar regions (figure 3). It was found that  $y(T_c)$  can be described with a Gaussian function (11), parameters of which have been evaluated.

The model was tested again through the simulation of the dielectric properties of relaxors using the obtained results for  $l$  and  $y(T_c)$ . The polar regions were treated as ferroelectrics with a second-order phase transition. It was shown that it was possible to have maxima in the temperature dependences of the real and imaginary parts of the dielectric permittivity for a finite frequency  $\omega$ , which are usually observed in the experiment. The peaks are caused by the effect of the slowing down of the relaxation time  $\tau$  of the polar regions. For individual regions,  $\tau$  increases on cooling below the local transition temperature as a result of increasing magnitude of the anisotropy energy density between the stable states (22) and decreasing thermal energy of the crystal. The width of the relaxation time spectrum  $g(z, T)$  becomes larger on cooling, also due to the increasing values of the relaxation times of the polar regions.

However, the model could not fully account for all the details of the frequency dependence of the dielectric properties. The calculated imaginary part of the dielectric permittivity differs markedly from that observed for relaxors (shown in figure 11d). The model also predicts that the relaxation time spectrum is a function monotonically decreasing with increasing  $\tau$ . At the same time, the experimental data [11] suggest that the spectrum has a maximum.

Two possible reasons for the disparities listed above can be pointed out: the use of a unique value of  $l$  in the calculations and/or the fact that the interaction between the polar regions was not taken into account. One can expect that the distribution of  $l$  plays a substantial role in the dynamic behaviour of relaxors. Although the distribution, either of the local transition temperature or the size of the polar regions, leads to frequency behaviour of the real part of the dielectric permittivity which is in good qualitative agreement with the experimental data, the latter seems to be more important. This is suggested by the comparison of the results of the present paper with those of the previous work. The model [7] with an unique transition temperature, but distribution of the size of the polar regions, yielded a behaviour of  $\varepsilon'(\omega, T)$  similar to the present model, but much better behaviour of  $\varepsilon''(\omega, T)$  [7] and the relaxation time spectrum [16].

## 9. Conclusions

The model for relaxors as superparaelectrics with a broad distribution of the local transition temperatures and a unique size of the polar regions has been investigated. It has been shown that the distribution can explain well the static polarization response and the real part of the dielectric permittivity of relaxors. However, the behaviour of the imaginary part of the dielectric permittivity and the relaxation time spectrum was not fully accounted for. It has been concluded that even though the model with a distribution of  $T_c$  but unique size reproduces qualitatively well some experimentally observed features of relaxors (the shift of the peaks in temperature dependence of the real and imaginary parts of the dielectric permittivity with frequency and broadening of the relaxation time spectrum on cooling), the distribution of the size of the polar regions seems to play a more important role in controlling the dynamic properties of relaxors.

### Acknowledgment

The authors gratefully acknowledge the Fonds National Suisse de la Recherche Scientifique for the financial support of this research.

### Appendix

The model presented in this paper assumes that it is the temperature  $T_c$  of the local phase transition which determines the difference in the values of dipole moments of individual polar regions. The function  $y(T_c)$  describes the distribution of the local transition temperatures of the polar regions. At a given temperature  $T$ , only the regions with  $T_c$  greater than  $T$  contribute to the orientation polarization  $P(T, E)$ . Therefore, the macroscopic polarization of the relaxor due to the alignment of the dipole moments of the polar regions parallel to the direction of the external electric field can be written in the form

$$P(T, E) = \int_T^\infty y(T_c) f(T, T_c, E) dT_c \quad (A1)$$

$$f(T, T_c, E) = P_s(T, T_c) \tanh\left(\frac{P_s(T, T_c) \cdot l^3 E}{3kT}\right).$$

The volume fraction (or the total number; for the present model this is the same, since the size of the polar regions,  $l$ , is constant) of the polar regions in the relaxor at temperature  $T$  is given by the value of  $Y(T)$ :

$$Y(T) = \int_T^\infty y(T_c) dT_c \quad (A2)$$

Equation (A1) may be rewritten as

$$P(T, E) = Y(T) \int_0^\infty h(T, T_c) f(T, T_c, E) dT_c \quad (A3)$$

where function  $h(T, T_c)$  is defined as

$$h(T, T_c) = \begin{cases} Y^{-1}(T)y(T_c) & T_c \geq T \\ 0 & T_c < T. \end{cases} \quad (A4)$$

In section 3 in order to facilitate the analysis of the experimental data we suggested substituting an ensemble of different regions by a system of identical ones, so the magnitude of the dipole moment is the same for all the regions. In terms of the local transition temperatures such a replacement means that all the polar regions have a unique temperature of the phase transition, which we denote as  $T^*$  (obviously,  $T^* > T$ ). Mathematically this may be expressed as the expansion of function  $h(T, T_c)$  in terms of delta function  $\delta(T_c - T^*)$ :

$$h(T, T_c) = a_0 \delta(T_c - T^*) + a_1 \frac{\partial \delta(T_c - T^*)}{\partial T_c} + \frac{a_2}{2} \frac{\partial^2 \delta(T_c - T^*)}{\partial T_c^2} + \dots \quad (A5)$$

This equation is similar to the expansion of the electric potential of the localized charge distribution in terms of multipoles. Coefficients  $a_0, a_1, a_2, \dots$  in (A5) may be found as

$$a_0 = \int_0^\infty h(T, T_c) dT_c = 1$$

$$a_1 = \int_0^\infty (T_c - T^*) h(T, T_c) dT_c \quad (A6)$$

$$a_2 = \int_0^\infty (T_c - T^*)^2 h(T, T_c) dT_c$$

etc.

They depend upon the temperature  $T$ ,  $T^*$  and a function  $h(T, T_c)$ . For brevity we terminated the expansion in (A5) at the third term. If we substitute now function  $h(T, T_c)$  from (A5) into equation (A3) we obtain

$$P(\mathbf{E}, T) = Y(T)f(T, T^*, \mathbf{E}) - a_1 Y(T) \left. \frac{\partial f(T, T_c, \mathbf{E})}{\partial T_c} \right|_{T_c=T^*} + \frac{a_2}{2} Y(T) \left. \frac{\partial^2 f(T, T_c, \mathbf{E})}{\partial T_c^2} \right|_{T_c=T^*}. \tag{A7}$$

We can rewrite it in the following form:

$$P(\mathbf{E}, T) = Y(T)f(T, T^*, \mathbf{E}) [1 - \delta_1 P + \delta_2 P] \tag{A8}$$

with  $\delta_1 P$  and  $\delta_2 P$  given by

$$\delta_1 P = \frac{a_1}{f(T, T^*, \mathbf{E})} \left. \frac{\partial f(T, T_c, \mathbf{E})}{\partial T_c} \right|_{T_c=T^*} \tag{A9}$$

$$\delta_2 P = \frac{a_2}{2f(T, T^*, \mathbf{E})} \left. \frac{\partial^2 f(T, T_c, \mathbf{E})}{\partial T_c^2} \right|_{T_c=T^*}.$$

The first term in (A7) and (A8) we use in section 5 to model the orientation polarization behaviour of the relaxor. We can write it explicitly:

$$P(\mathbf{E}, T) = Y(T)P_s(T, T^*) \tanh \left( \frac{P_s(T, T^*) \cdot l^3 \mathbf{E}}{3kT} \right). \tag{A10}$$

Two others,  $\delta_1 P$  and  $\delta_2 P$ , will be considered as the errors brought about by the replacement of an ensemble of the polar regions.

Function  $f(T, T_c, \mathbf{E})$  is a complicated non-linear function of  $T_c$ ; it depends explicitly on  $P_s$ , which, in turn, depends upon  $T_c$ . We can simplify the expressions for  $\delta_1 P$  and  $\delta_2 P$  in the following way. For example, we can modify the expression for  $\delta_1 P$  as

$$\delta_1 P = \frac{a_1}{f(T^*)} \left. \frac{\partial f}{\partial T_c} \right|_{T_c=T^*} = \frac{a_1}{f(T^*)} \left. \frac{\partial f}{\partial P_s} \frac{\partial P_s}{\partial T_c} \right|_{T_c=T^*} = \frac{a_1}{P_s} \left. \frac{\partial P_s}{\partial T_c} \right|_{T_c=T^*} \left\{ \left. \frac{\partial f}{\partial P_s} \right|_{T_c=T^*} \frac{P_s}{f(T^*)} \right\}. \tag{A11}$$

For a given temperature  $T$ , the magnitude of the expression in the curly brackets depends upon the value of the applied field  $\mathbf{E}$ . It is straightforward to show that its absolute value is limited to two. Therefore, we can obtain that

$$\delta_1 P \leq 2 \frac{a_1}{P_s} \left. \frac{\partial P_s}{\partial T_c} \right|_{T_c=T^*}. \tag{A12}$$

In the same way one can show that  $\delta_2 P$  is limited by

$$\delta_2 P = a_2 \left( \frac{\theta_1}{P_s^2} \left( \frac{\partial P_s}{\partial T_c} \right)^2 + \frac{\theta_2}{P_s} \frac{\partial^2 P_s}{\partial T_c^2} \right) \Big|_{T_c=T^*}. \tag{A13}$$

Coefficients  $\theta_1$  and  $\theta_2$  come from expressions similar to that given in the curly brackets in (A11):

$$\theta_1 = \left. \frac{\partial^2 f}{\partial P_s^2} \right|_{T_c=T^*} \frac{P_s^2}{f(T^*)} \quad \theta_2 = \left. \frac{\partial f}{\partial P_s} \right|_{T_c=T^*} \frac{P_s}{f(T^*)}.$$



They both are positive values, smaller than two.

When we know the temperature dependence of the spontaneous polarization  $P_s$  of the model ferroelectric, the function  $y(T_c)$  and the value of  $T^*$ , we can estimate the magnitudes of the correction terms and evaluate the precision of the model.

In the case of a ferroelectric with a second-order phase transition which has a low-temperature phase with a rhombohedral structure the temperature dependence of the spontaneous polarization is given by equation (22) (section 7):

$$P_s^2 = \frac{3\alpha_1(T_c - T)}{2(\alpha_{11} + \alpha_{12})}.$$

Therefore, from (A12) and (A13) one may easily obtain expressions for the estimates of the errors:

$$\begin{aligned} \delta_1 P &\leq \frac{a_1}{T^* - T} \\ \delta_2 P &\leq \frac{a_2(\theta_1 - \theta_2)}{8(T^* - T)^2}. \end{aligned} \tag{A14}$$

For a ferroelectric with a second-order phase transition the magnitudes of  $\delta_1 P$  and  $\delta_2 P$  do not depend on the values of the free energy coefficients.

## References

- [1] Smolensky G A, Isupov V A, Agranovskaya A I and Popov S N 1961 *Sov. Phys.-Solid State* **2** 2584
- [2] Bokov V A and Myl'nikova I E 1961 *Sov. Phys.-Solid State* **3** 613
- [3] Smolensky G A 1970 *J. Phys. Soc. Japan Suppl.* **26** **28**
- [4] Kirillov V V and Isupov V A 1973 *Ferroelectrics* **5** 3
- [5] Cross L E 1987 *Ferroelectrics* **76** 241
- [6] Viehland D, Li J F, Jang S J, Cross L E and Wuttig M 1991 *Phys. Rev. B* **43** 8316
- [7] Bell A J 1993 *J. Phys.: Condens. Matter* **5** 8773
- [8] Bell A J and Glazounov A E 1994 *Br. Ceram. Proc.* **52** 29
- [9] Dorogovtsev S N and Yushin N K 1990 *Ferroelectrics* **112** 27
- [10] Viehland D, Jang S J, Cross L E and Wuttig M 1990 *J. Appl. Phys.* **68** 2916
- [11] Colla E V, Koroleva E Yu, Okuneva N M and Vakhrushev S B 1992 *J. Phys.: Condens. Matter* **4** 3671
- [12] de Mathan N, Husson E, Calvarin G, Gavarrri J R, Hewat A W and Morell A 1991 *J. Phys.: Condens. Matter* **3** 8159
- [13] Von Hippel A 1954 1993 *Dielectrics and Waves* (Cambridge, MA: MIT Press)
- [14] Butcher S J and Daghish M 1993 *Third Euro-Ceramics, Proc. 3rd European Ceramic Soc. Conf. (Madrid, 1993)* vol 2 (Faenza: Editrice Iberica) p 121
- [15] Haun M J, Zhang Z Q, Furman E, Jang S J and Cross L E 1989 *Ferroelectrics* **99** 45
- [16] Bell A J 1994 unpublished